



The Crystal Structures of Two Hydro-*closo*-Borates with Divalent Tin in Comparison: $\text{Sn}(\text{H}_2\text{O})_3[\text{B}_{10}\text{H}_{10}] \cdot 3 \text{H}_2\text{O}$ and $\text{Sn}(\text{H}_2\text{O})_3[\text{B}_{12}\text{H}_{12}] \cdot 4 \text{H}_2\text{O}$

Fabian M. Kleeberg¹ · Lucas W. Zimmermann¹ · Thomas Schleid¹

Received: 5 August 2021 / Accepted: 20 August 2021 / Published online: 13 September 2021
© The Author(s) 2021

Abstract

Single crystals of $\text{Sn}(\text{H}_2\text{O})_3[\text{B}_{10}\text{H}_{10}] \cdot 3 \text{H}_2\text{O}$ and $\text{Sn}(\text{H}_2\text{O})_3[\text{B}_{12}\text{H}_{12}] \cdot 4 \text{H}_2\text{O}$ are easily accessible by reactions of aqueous solutions of the acids $(\text{H}_3\text{O})_2[\text{B}_{10}\text{H}_{10}]$ and $(\text{H}_3\text{O})_2[\text{B}_{12}\text{H}_{12}]$ with an excess of tin metal powder after isothermal evaporation of the clear brines. Both compounds crystallize with similar structures in the triclinic system with space group $P \bar{1}$ and $Z = 2$. The crystallographic main features are electroneutral $\frac{1}{\infty} \{ \text{Sn}(\text{H}_2\text{O})_{3/1}[\text{B}_{10}\text{H}_{10}]_{3/3} \}$ and $\frac{1}{\infty} \{ \text{Sn}(\text{H}_2\text{O})_{3/1}[\text{B}_{12}\text{H}_{12}]_{3/3} \}$ double chains running along the a -axes. Each Sn^{2+} cation is coordinated by three water molecules of hydration ($d(\text{Sn}-\text{O}) = 221\text{--}225$ pm for the B_{10} and $d(\text{Sn}-\text{O}) = 222\text{--}227$ pm for the B_{12} compound) and additionally by hydridic hydrogen atoms of the three nearest boron clusters ($d(\text{Sn}-\text{H}) = 281\text{--}322$ pm for the B_{10} and $d(\text{Sn}-\text{H}) = 278\text{--}291$ pm for the B_{12} compound), which complete the coordination sphere. Between these tin(II)-bonded water and the three or four interstitial crystal water molecules, classical bridging hydrogen bonds are found, connecting the double chains to each other. Furthermore, there is also *non*-classical hydrogen bonding between the anionic $[\text{B}_n\text{H}_n]^{2-}$ ($n = 10$ and 12) clusters and the crystal water molecules pursuant to $\text{B}-\text{H}^{\delta-} \cdots \delta^+\text{H}-\text{O}$ interactions often called dihydrogen bonds.

Keywords Divalent tin · Lone-pair cations · Decahydro-*closo*-decaborates · Dodecahydro-*closo*-dodecaborates · Hydrates

Introduction

Interactions between soft metal cations, e.g. Cu^+ , Ag^+ and Hg^{2+} , and hydro-*closo*-borate anions $[\text{B}_n\text{H}_n]^{2-}$ ($n = 10$ and 12) were firstly discussed in the 1960s [1]. The salt-like copper(I) compound $\text{Cu}_2[\text{B}_{10}\text{H}_{10}]$ shows $\text{Cu} \cdots \text{B}$ distances in the range from 214 to 233 pm, indicating a covalent interaction between the Cu^+ cation and the hydro-*closo*-borate anion which was suggested as a three-centered two-electron $\text{Cu}-\text{H}-\text{B}$ bond [2]. This assumption was encouraged by the infrared spectra, which unveils two distinct absorption bands in the $\text{B}-\text{H}$ stretching area, one for the non-coordinating BH groups and another for the BH groups entailed in the $\text{Cu}-\text{H}-\text{B}$ interactions [3]. Similar can be found in the infrared spectra of the compounds $[\text{Cu}_2(\text{bpa})_2\text{B}_{10}\text{H}_{10}]$ and $[\text{Cu}_2(\text{bpa})_2(\text{OH})_2]_2[\text{Cu}_2(\text{B}_{10}\text{H}_{10})_3] \cdot n$

CH_3CN , both revealing stretching vibrations of BH groups in three-centered $\text{Cu}-\text{H}-\text{B}$ bonds. Additionally the X-ray crystal structure of $[\text{Cu}_2(\text{bpa})_2(\text{OH})_2\text{B}_{10}\text{H}_{10}]$ shows $\text{Cu}-\text{H}$ contacts in the range of 263–273 pm [4]. For the higher homologous salt-like silver(I) compound $\text{Ag}_2[\text{B}_{10}\text{H}_{10}]$ [1, 5], up to now, no crystal structure could be determined, but the presence of three-centered $\text{Ag}-\text{H}-\text{B}$ is supported by infrared spectroscopic data [5]. In the further case of Cu^+ and Ag^+ cations the review article by Avdeeva et al. [6] should be mentioned, as it provides a good overview of this field.

Up to now, these kind of connections can be found in several other salt-like hydro-*closo*-borates, especially with cations of the 6th period possessing *lone-pair* electrons. All of these compounds unveil interesting properties. The thallium(I) salt $\text{Tl}_2[\text{B}_{12}\text{H}_{12}]$ [7] exhibits a yellow metal-centered luminescence at room temperature, based on an apparent covalent interaction between Tl^+ and the hydridic hydrogen atoms of the $[\text{B}_{12}\text{H}_{12}]^{2-}$ anions [8]. Besides $\text{Tl}_2[\text{B}_{12}\text{H}_{12}]$, there can be also found two lead(II) dodecahydro-*closo*-dodecaborates, $\text{Pb}[\text{B}_{12}\text{H}_{12}]$ [9] with a pure

✉ Thomas Schleid
schleid@iac.uni-stuttgart.de

¹ Institut für Anorganische Chemie, Universität Stuttgart, Pfaffenwaldring 55, 70569 Stuttgart, Germany

$6s^2$ nature of the non-bonding electron *lone pair*, and $\text{Pb}(\text{H}_2\text{O})_3[\text{B}_{12}\text{H}_{12}] \cdot 3 \text{H}_2\text{O}$ [7], where each Pb^{2+} cation shows an irregular coordination sphere, indicating a *lone pair* with increased *p* character and thus stereochemical activity. In the dimeric compound $[\text{Pb}(\text{bipy})_2(\text{B}_{12}\text{H}_{12})]_2$, the lead(II) cations are coordinated by two bipyridyl molecules and via faces to two $[\text{B}_{12}\text{H}_{12}]^{2-}$ dianions, showing Pb–H contacts in the range of 279–307 pm [10], indicating a $6s^2$ nature of the non-bonding electron *lone pair*.

For the homologous decahydro-*closo*-decaborate anions $[\text{B}_{10}\text{H}_{10}]^{2-}$, interactions between these anions and cations with *lone-pair* electrons were expected. They could be verified through two lead(II) decahydro-*closo*-decaborates $[\text{Pb}(\text{H}_2\text{O})_3]_2\text{Pb}[\text{B}_{10}\text{H}_{10}]_3 \cdot 5.5 \text{H}_2\text{O}$ and $[\text{Pb}(\text{H}_2\text{O})_3]\text{Pb}[\text{B}_{10}\text{H}_{10}]_2 \cdot 1.5 \text{H}_2\text{O}$ [11] with different water content, which display hydrated Pb^{2+} cations each, but also cations only coordinated by hydridic hydrogen atoms of the boron cluster anions, as well as through the complex $[\text{Pb}(\text{bipy})\text{B}_{10}\text{H}_{10}]$ [10, 12]. Herein the Pb^{2+} cation is surrounded *quasi*-tetrahedrally by three $[\text{B}_{10}\text{H}_{10}]^{2-}$ ($d(\text{Pb}-\text{H}) = 266\text{--}318 \text{ pm}$) anions and the neutral bipyridyl ligand. As in the lead compound just mentioned above, in the thallium(I) salt $\text{Tl}_2[\text{B}_{10}\text{H}_{10}]$ [13] all Tl^+ cations are only coordinated by hydridic hydrogen atoms of the boron cluster anions. This compound crystallizes isotypically with the salt-like decahydro-*closo*-decaborates of some alkali metals ($A = \text{Na}, \text{K}$ and Rb) [14], but with marked differences in the $\text{Tl} \cdots \text{H}$ coordination spheres, based on stereochemically active *lone-pair* electrons. All these compounds can be seen as potential precursors for metalated boron clusters such as $[\text{Et}_3\text{N}][\text{Cu}(1\text{-B}_{10}\text{H}_9\text{N}_2)_2]$ ($d(\text{Cu}-\text{B}) = 218 \text{ pm}$) [15], $[\text{P}(\text{C}_6\text{H}_5)_4]_2[2\text{-SnCl}(\text{C}_6\text{H}_5)_2\text{-B}_{10}\text{H}_9]$ and $[\text{P}(\text{C}_6\text{H}_5)_4]_2[2\text{-SnCl}_2(\text{C}_6\text{H}_5)\text{B}_{10}\text{H}_9]$ ($d(\text{Sn}-\text{B}) = 217\text{--}219 \text{ pm}$) [16, 17], eventually leading to features like in the recently published neutral molecule $[\text{BiB}_{12}\text{H}_{11}]$ with a covalent Bi–B single bond ($d(\text{Bi}-\text{B}) = 230 \text{ pm}$) manifesting an inverted polarity as compared to the typical B–H bonds [18, 19].

Results and Discussion

The newly synthesized triaqua-tin(II) decahydro-*closo*-decaborate trihydrate crystallizes in the triclinic space group $P \bar{1}$ with $a = 756.49(5) \text{ pm}$, $b = 948.47(6) \text{ pm}$, $c = 1034.52(7) \text{ pm}$, $\alpha = 69.141(2)^\circ$, $\beta = 85.364(2)^\circ$, $\gamma = 87.258(2)^\circ$ as lattice parameters and two formula units per unit cell (Tables 1 and 2) [20].

The crystallographically unique Sn^{2+} cation is coordinated by three oxygen atoms (O1–O3) from the corresponding water molecules of hydration forming the first

coordination sphere with $d(\text{Sn}-\text{O}) = 221\text{--}225 \text{ pm}$ (Fig. 1, left). This coordination polyhedron can be interpreted as non-planar $[\text{Sn}(\text{H}_2\text{O})_3]^{2+}$ cation, structurally very similar to the complex $[\text{Pb}(\text{H}_2\text{O})_3]^{2+}$ cations ($d(\text{Pb}-\text{O}) = 242\text{--}252 \text{ pm}$) known from the lead(II) containing hydro-*closo*-borate hydrates [7, 11]. Furthermore, a second coordination sphere is built up by three decahydro-*closo*-decaborate anions in such a way, that two of these three $[\text{B}_{10}\text{H}_{10}]^{2-}$ clusters interact via their triangular faces and a third one via a single corner with each tin(II) cation. Together with the three water molecules of hydration they erect a distorted trigonal antiprism with their barycenters providing for $\text{CN} = 10$ ($3 \times \text{O} + 7 \times \text{H}$) as overall coordination number (Fig. 1, right). This asymmetric coordination of the Sn^{2+} cation by the three boron clusters allows space for the stereochemically active $5sp$ *lone pair* of electrons. The corresponding Sn–H distances range from 281 to 322 pm and are in good accordance with the already known decahydro-*closo*-decaborates containing *lone-pair* cations with significant hydrogen interactions, e.g. $[\text{Pb}(\text{H}_2\text{O})_3]_2\text{Pb}[\text{B}_{10}\text{H}_{10}]_3 \cdot 5.5 \text{H}_2\text{O}$ with $d(\text{Pb}-\text{H}) = 249\text{--}285 \text{ pm}$ [11].

Each $[\text{B}_{10}\text{H}_{10}]^{2-}$ anion consists of ten independent boron and hydrogen atoms each with B–B distances between 181 and 185 pm within the square antiprism, but 169–171 pm to the apical boron atoms, and B–H distances from 104 to 116 pm. All these distances indicate only minor distortions from the ideal symmetry as bicapped square antiprism, caused by anisotropic direct interactions of three Sn^{2+} cations attached to each boron cluster. Due to these connections of every $[\text{B}_{10}\text{H}_{10}]^{2-}$ anion with three tin(II) cations the structure is built up by electroneutral double chains with the formula ${}^1_{\infty}\{\text{Sn}(\text{H}_2\text{O})_{3/1}[\text{B}_{10}\text{H}_{10}]_{3/3}\}$ (Fig. 2) running along the *a*-axis. These double strands are interconnected with each other through three interstitial water molecules (O4w–O6w), which are bonded via classical $\text{O}-\text{H}^{\delta+} \cdots \delta^-\text{O}$ hydrogen bonds to the tin(II)-coordinated water molecules of hydration (O1–O3).

The interatomic $\text{O} \cdots \text{H}$ distances for these hydrogen bonds range from 171 to 189 pm and can be classified as decently strong, whereas the hydrogen bond interactions among the crystal water molecules O4w and O6w with H42w \cdots O6w distances of 217 pm are rather weak (Fig. 3, left) [21]. Beneath the classical hydrogen bonds, also *unconventional* hydrogen-bonds $\text{B}-\text{H}^{\delta-} \cdots \delta^+\text{H}-\text{O}$ [22] can be observed (Fig. 3, right). These non-classical so-called *dihydrogen bonds* occur between the negatively polarized hydrogen atoms of the $[\text{B}_{10}\text{H}_{10}]^{2-}$ anions and the protonic hydrogen atoms of the H_2O molecules with $d(\text{H}^{\delta-} \cdots \delta^+\text{H}) = 186\text{--}225 \text{ pm}$. Each $[\text{B}_{10}\text{H}_{10}]^{2-}$ anion builds up non-classical hydrogen bonds to the nearest water molecules, represented by O3, O4w, O5w ($2 \times$) and O6w

Table 1 Crystallographic data for $\text{Sn}(\text{H}_2\text{O})_3[\text{B}_{10}\text{H}_{10}] \cdot 3 \text{H}_2\text{O}$ and $\text{Sn}(\text{H}_2\text{O})_3[\text{B}_{12}\text{H}_{12}] \cdot 4 \text{H}_2\text{O}$

Empirical formula	$\text{Sn}(\text{H}_2\text{O})_3[\text{B}_{10}\text{H}_{10}] \cdot 3 \text{H}_2\text{O}$	$\text{Sn}(\text{H}_2\text{O})_3[\text{B}_{12}\text{H}_{12}] \cdot 4 \text{H}_2\text{O}$
Crystal system	triclinic	
Space group	$P \bar{1}$ (no. 2)	
Lattice constants		
a/pm	756.49(5)	741.72(5)
b/pm	948.47(6)	991.56(7)
c/pm	1034.52(7)	1154.63(8)
$\alpha/^\circ$	69.141(2)	74.471(2)
$\beta/^\circ$	85.364(2)	83.430(2)
$\gamma/^\circ$	87.258(2)	87.483(2)
Number of formula units, Z	2	
Calculated density, $D_x/\text{g cm}^{-3}$	1.657	1.580
Molar volume, $V_m/\text{cm}^3 \text{ mol}^{-1}$	208.19	244.70
Measuring diffractometer	κ -CCD (Bruker Nonius)	
Radiation	$\text{Mo-}K_\alpha$ ($\lambda = 71.07 \text{ pm}$)	
Measuring temperature	100 K	
Measurement limit, $\Theta_{\text{max}}/^\circ$	27.88	28.37
Index ranges	9/12/13	9/13/15
$F(000)$	340	384
Absorption coefficient, μ/mm^{-1}	1.847	1.583
Data corrections	Empirical, Program Scalepack	
Number of measured reflections	6043	7869
Number of unique reflections	3278	4047
Structure solution and refinement	Programs SHELXS-97 and SHELXL-97	
$R_{\text{int}} / R_\sigma$	0.031 / 0.044	0.036 / 0.058
R_1 for (n) reflections with $ F_o \geq 4\sigma(F_o)$	0.024 (2890)	0.027 (3439)
R_1 / wR_2 for all reflections	0.032 / 0.046	0.037 / 0.041
GooF	1.037	0.958
Residual electron density, $\rho/e^- \times 10^{-6} \text{ pm}^{-3}$, min. / max.	- 0.53 / 0.61	- 0.43 / 0.54

(2 ×), from which O3 is coordinated directly to a tin(II) cation as water molecule of hydration and the other oxygen atoms stand for free interstitial crystal water molecules (Fig. 4).

The higher homologous dodecaborate with the composition $\text{Sn}(\text{H}_2\text{O})_3[\text{B}_{12}\text{H}_{12}] \cdot 4 \text{H}_2\text{O}$ crystallizes also in the triclinic space group $P \bar{1}$ with $a = 741.72(5) \text{ pm}$, $b = 991.56(7) \text{ pm}$, $c = 1154.63(8) \text{ pm}$, $\alpha = 74.471(2)^\circ$, $\beta = 83.430(2)^\circ$, $\gamma = 87.483(2)^\circ$ for two formula units per unit cell (Tables 1 and 3) [13]. The unique Sn^{2+} cation is surrounded by three water molecules of hydration (O1–O3, $d(\text{Sn–O}) = 222\text{–}224 \text{ pm}$) again, leading to the already mentioned $[\text{Sn}(\text{H}_2\text{O})_3]^{2+}$ cation, and three icosahedral $[\text{B}_{12}\text{H}_{12}]^{2-}$ cluster anions are attached via only one hydrogen atom of each cage ($d(\text{Sn–H}) = 273\text{–}281 \text{ pm}$) providing for a total coordination number of six for the first coordination sphere of the divalent tin (Fig. 5, left). The irregular arrangement of the three oxygen and three

hydrogen atoms leaves enough space for a 5sp lone pair of electrons with stereochemical activity. Further tin-hydrogen distances can be found in the range of 315–333 pm, so each of the three boron cages finally coordinates via one triangular face to every Sn^{2+} cation with a total coordination number of 12 for the first and second coordination sphere (Fig. 5, right).

A similar structural motif can be found in the orthorhombic lead(II) salt $\text{Pb}(\text{H}_2\text{O})_3[\text{B}_{12}\text{H}_{12}] \cdot 3 \text{H}_2\text{O}$, also showing stereochemically active lone pairs (6sp) at the Pb^{2+} cations and direct metal-to-hydrogen interactions ($d(\text{Pb–H}) = 257\text{–}338 \text{ pm}$) [7]. Each quasi-icosahedral $[\text{B}_{12}\text{H}_{12}]^{2-}$ anion is built up from twelve crystallographically independent boron and hydrogen atoms each ($d(\text{B–B}) = 177\text{–}180 \text{ pm}$, $d(\text{B–H}) = 106\text{–}114 \text{ pm}$) and shows only minor deviations from the ideal values of 178 pm for $d(\text{B–B})$ and 110 pm for $d(\text{B–H})$ for these types of bonds [23]. The pyramidal $[\text{Sn}(\text{H}_2\text{O})_3]^{2+}$ units are interconnected

Table 2 Atomic positions and equivalent isotropic displacement coefficients for $\text{Sn}(\text{H}_2\text{O})_3[\text{B}_{10}\text{H}_{10}] \cdot 3 \text{H}_2\text{O}$ (all atoms occupy the general *Wyckoff* position *2i*)

Atom	<i>x/a</i>	<i>y/b</i>	<i>z/c</i>	$U_{\text{eq}}/\text{pm}^2$
Sn	0.26718(2)	0.584223(18)	0.195601(17)	93(5)
O1	0.0601(2)	0.75424(18)	0.20138(19)	108(3)
H11	0.032(5)	0.741(4)	0.274(4)	370(11)
H12	0.961(5)	0.768(4)	0.155(4)	440(10)
O2	0.4224(2)	0.7584(2)	0.22910(18)	115(3)
H21	0.530(5)	0.775(4)	0.193(3)	310(9)
H22	0.382(4)	0.837(4)	0.205(3)	280(9)
O3	0.2065(5)	0.5261(2)	0.42537(17)	121(3)
H31	0.265(5)	0.559(4)	0.465(4)	440(11)
H32	0.185(5)	0.437(5)	0.466(4)	570(13)
O4w	0.7472(2)	0.7692(2)	0.0936(2)	134(3)
H41w	0.742(4)	0.682(4)	0.084(4)	380(10)
H42w	0.736(5)	0.824(4)	0.024(4)	310(10)
O5w	0.1078(3)	0.2362(2)	0.55985(18)	143(3)
H51w	0.187(5)	0.180(4)	0.576(3)	390(9)
H52w	0.047(5)	0.216(4)	0.508(4)	340(10)
O6w	0.2757(2)	0.0365(2)	0.17935(19)	143(3)
H61w	0.330(5)	0.083(4)	0.216(3)	320(9)
H62w	0.176(5)	0.034(4)	0.212(4)	400(10)
B1	0.6329(3)	0.3950(3)	0.3255(3)	105(5)
H1	0.571(4)	0.483(3)	0.370(3)	190(7)
B2	0.5362(3)	0.2594(3)	0.2862(3)	105(5)
H2	0.395(4)	0.248(3)	0.305(3)	300(8)
B3	0.6727(3)	0.4073(3)	0.1577(3)	93(5)
H3	0.646(4)	0.507(3)	0.069(3)	150(7)
B4	0.8482(3)	0.3658(3)	0.27771(3)	96(5)
H4	0.948(3)	0.438(3)	0.290(3)	130(7)
B5	0.7130(3)	0.2168(3)	0.4067(3)	117(5)
H5	0.713(4)	0.166(3)	0.519(3)	200(7)
B6	0.6494(3)	0.2284(3)	0.1364(3)	93(5)
H6	0.576(4)	0.228(3)	0.050(3)	280(8)
B7	0.8717(3)	0.3028(3)	0.1304(3)	91(5)
H7	0.966(4)	0.354(3)	0.042(3)	200(7)
B8	0.8985(3)	0.1678(3)	0.3066(3)	102(5)
H8	0.016(4)	0.113(3)	0.356(3)	190(7)
B9	0.6782(3)	0.0929(3)	0.3113(3)	110(5)
H9	0.616(4)	0.980(3)	0.366(3)	240(8)
B10	0.8327(3)	0.1151(3)	0.1773(3)	106(5)
H10	0.894(3)	0.033(3)	0.133(3)	140(7)

via $[\text{B}_{12}\text{H}_{12}]^{2-}$ anions to form electroneutral double chains again, now with the formula ${}^1_{\infty}\{\text{Sn}(\text{H}_2\text{O})_{3/1}[\text{B}_{12}\text{H}_{12}]_{3/3}\}$, which run parallel to the *a*-axis (Fig. 6). These double chains get connected to each other through the four

remaining interstitial crystal water molecules (O4w–O7w) erecting the layer structure of $\text{Sn}(\text{H}_2\text{O})_3[\text{B}_{12}\text{H}_{12}] \cdot 4 \text{H}_2\text{O}$.

These interstitial crystal water molecules are bonded via strong classical $\text{O}-\text{H}^{\delta+} \cdots \delta-\text{O}$ hydrogen bonds ($d(\text{O}-\text{H} \cdots \text{O}) = 175\text{--}221 \text{ pm}$, $\angle(\text{O}-\text{H} \cdots \text{O}) = 153\text{--}174^\circ$) to the tin(II)-attached water molecules of hydration (O1–O3; Fig. 7, left). Furthermore, the hydridic hydrogen atoms of the $[\text{B}_{12}\text{H}_{12}]^{2-}$ anions interact with the protonic hydrogen atoms of the water molecules of hydration. Each $[\text{B}_{12}\text{H}_{12}]^{2-}$ anion forms six strong non-classical hydrogen bonds with the nearest water molecules, represented by O2, O4w (2 ×), O5w and O6w (2 ×), with $\text{H}^{\delta-} \cdots \text{H}^{\delta+}$ distances ranging from 191 to 225 pm (Fig. 7, right, and Fig. 8).

Vibrational Spectroscopy

Despite the two different boron clusters the infrared (IR) and *Raman* spectra of both compounds are very similar to each other (Fig. 9) and all observed peaks could be assigned successfully. The O–H stretching bands at 3596, 3523 and 3440 cm^{-1} are broadened due to hydrogen bonds ($\text{O}-\text{H}^{\delta+} \cdots \text{O}^{\delta-}$) between the tin(II)-coordinating water molecules of hydration and the free interstitial crystal water molecules.

For the B–H stretching modes between 2400 and 2550 cm^{-1} , there can be found peaks in all four spectra. The sharp peaks in the *Raman* spectra show no hint for any non-classical hydrogen bonds ($\text{B}-\text{H}^{\delta-} \cdots \delta+\text{H}-\text{O}$), whereas the infrared spectra of $\text{Sn}(\text{H}_2\text{O})_3[\text{B}_{10}\text{H}_{10}] \cdot 3 \text{H}_2\text{O}$ exhibit a band at 2470 cm^{-1} with a distinct shoulder at 2517 cm^{-1} and a broad band covering an interval from 2400 to 1800 cm^{-1} . The infrared spectra of $\text{Sn}(\text{H}_2\text{O})_3[\text{B}_{12}\text{H}_{12}] \cdot 4 \text{H}_2\text{O}$ displays a sharp band at 2491 cm^{-1} , with a slight shoulder at 2521 cm^{-1} and only a weakly broadening between 2390 and 2380 cm^{-1} . The splitting of the B–H stretching mode in a low-frequency and high-frequency region is caused by B–H groups participating in hydrogen bonding (low-frequency shift) and groups that do not participate in hydrogen bonding (high-frequency shift). This clearly signaling the presence of non-classical hydrogen bonds [24].

Possible occurring B–H \cdots Sn stretching vibrations are expected in the low field at 2100 to 2000 cm^{-1} [25, 26], which is debatable for $\text{Sn}(\text{H}_2\text{O})_3[\text{B}_{10}\text{H}_{10}] \cdot 3 \text{H}_2\text{O}$, but an existing peak might be covered, whereas the IR spectra of $\text{Sn}(\text{H}_2\text{O})_3[\text{B}_{12}\text{H}_{12}] \cdot 4 \text{H}_2\text{O}$ shows no indication of this.

Furthermore, the H–O–H bending vibrations can also be observed in all the spectra. While the IR spectra show sharp bands at 1626 and 1607 cm^{-1} , in the *Raman* spectra there are just superficial peaks appearing at 1605 and 1602 cm^{-1} . Also the peaks in the O–H bending area reveal a slight broadening in the IR spectra, indicating classical

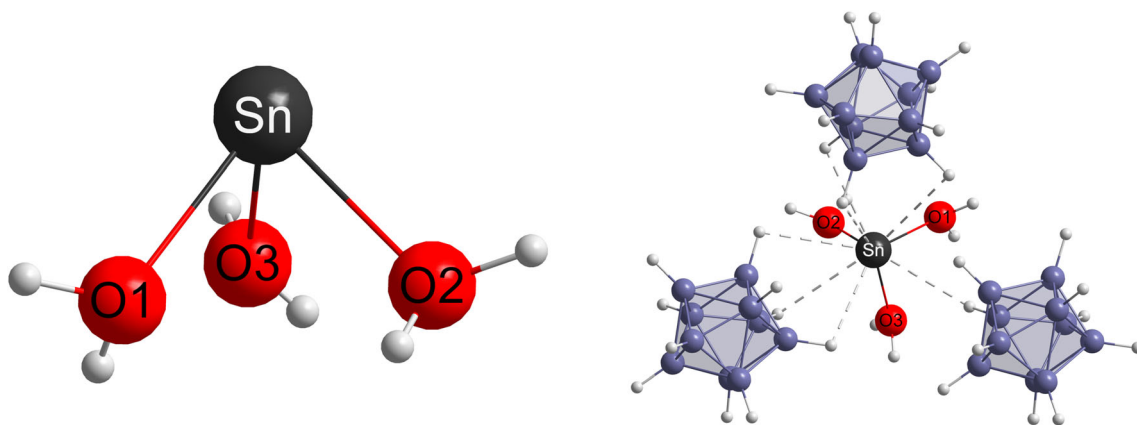


Fig. 1 Coordination of the Sn^{2+} cation by three water molecules of hydration (left) and its second coordination sphere recruited of three additional $[\text{B}_{10}\text{H}_{10}]^{2-}$ anions (right) in the crystal structure of $\text{Sn}(\text{H}_2\text{O})_3[\text{B}_{10}\text{H}_{10}] \cdot 3 \text{H}_2\text{O}$

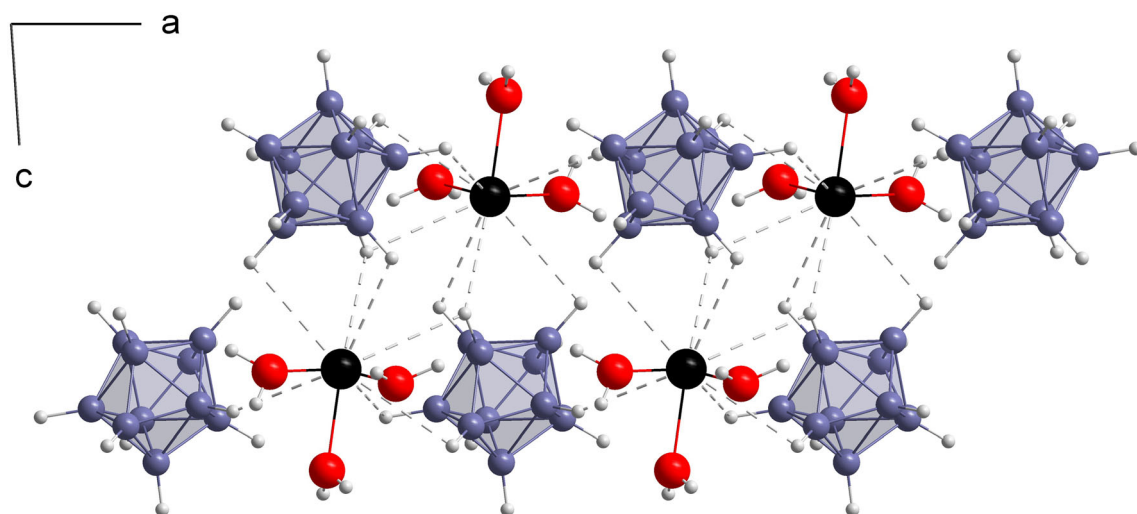


Fig. 2 Electroneutral double chain with the formula $\frac{1}{\infty} \{ \text{Sn}(\text{H}_2\text{O})_{3/1} [\text{B}_{10}\text{H}_{10}]_{3/3} \}$ in triclinic $\text{Sn}(\text{H}_2\text{O})_3[\text{B}_{10}\text{H}_{10}] \cdot 3 \text{H}_2\text{O}$ propagating parallel to the a -axis as viewed along $[010]$

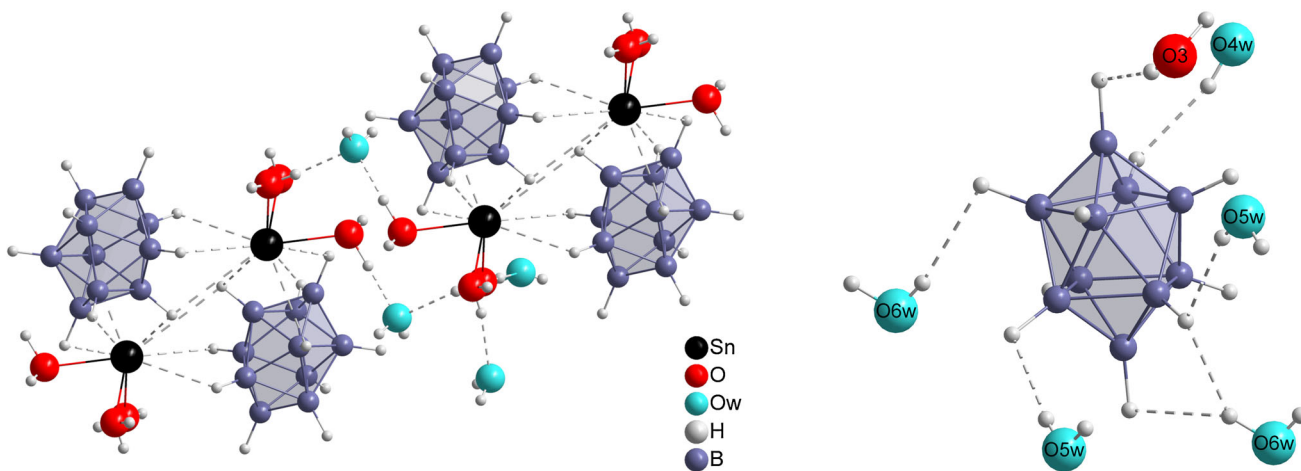


Fig. 3 Classical (left) and non-classical hydrogen bonds (right) in $\text{Sn}(\text{H}_2\text{O})_3[\text{B}_{10}\text{H}_{10}] \cdot 3 \text{H}_2\text{O}$

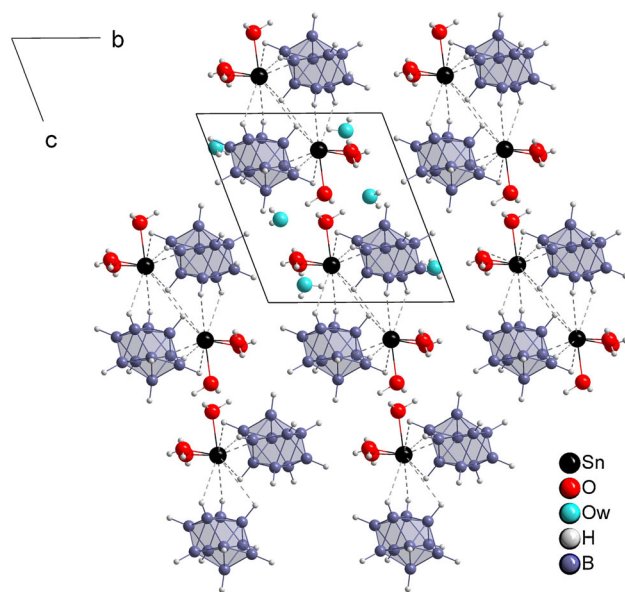


Fig. 4 Crystal structure of $\text{Sn}(\text{H}_2\text{O})_3[\text{B}_{10}\text{H}_{10}] \cdot 3 \text{H}_2\text{O}$ as viewed along the a -axis as quasi-hexagonal rod-packing of ${}^1_{\infty}\{\text{Sn}(\text{H}_2\text{O})_{3/1}[\text{B}_{10}\text{H}_{10}]_{3/3}\}$ double chains, held together by the interstitial water molecules (H_2O_w)

and *non*-classical hydrogen bonds. The remaining signals encountered in the IR spectra at 1079, 1025, 878 and 713 cm^{-1} can be assigned to B–B stretching vibrations, also visible in the Raman spectra at 1007, 998, 737, 616 and 580 cm^{-1} . The very intense peaks at 835 and 744 cm^{-1} are caused by the total symmetric breathing modes of the B_{10} and B_{12} cages.

Conclusion

Two tin(II) hydro-*closo*-borate hydrates were accessible from reactions of elemental tin with aqueous solutions of the acids $(\text{H}_3\text{O})_2[\text{B}_{10}\text{H}_{10}]$ and $(\text{H}_3\text{O})_2[\text{B}_{12}\text{H}_{12}]$. Both compounds crystallize in the same triclinic space group ($P\bar{1}$) with $Z = 2$ and differ only slightly in structure and composition. In both compounds the Sn^{2+} cations are coordinated by three oxygen atoms of the corresponding water molecules of hydration, building up *non*-planar $[\text{Sn}(\text{H}_2\text{O})_3]^{2+}$ units with Sn–O distances in an interval of 221 to 225 pm and a 151 pm off-center shift. Furthermore, three $[\text{B}_{10}\text{H}_{10}]^{2-}$ and $[\text{B}_{12}\text{H}_{12}]^{2-}$ cluster anions establish a second coordination sphere with tin(II)-hydrogen contacts ($d(\text{Sn}-\text{H}) = 273\text{--}333 \text{ pm}$), providing enough space for the stereochemically active $5s$ lone pair of electrons. The Sn^{2+} cations unveil a coordination behavior very similar to that of the heavier congener Pb^{2+} in its hydrated hydro-*closo*-borate compounds. Even the metal hydrogen contacts are in the same range ($d(\text{Pb}-\text{H}) = 249\text{--}338 \text{ pm}$) [7, 11]. But in comparison, the Sn–H distances are substantially

Table 3 Atomic positions and equivalent isotropic displacement coefficients for $\text{Sn}(\text{H}_2\text{O})_3[\text{B}_{12}\text{H}_{12}] \cdot 4 \text{H}_2\text{O}$ (all atoms occupy the general Wyckoff position $2i$)

Atom	x/a	y/b	z/c	$U_{\text{eq}} / \text{pm}^2$
Sn	0.21607(2)	0.870397(15)	0.701266(14)	123(5)
O1	0.0427(2)	0.68534(17)	0.72700(15)	140(3)
H11	0.966(3)	0.696(2)	0.698(2)	60(7)
H12	0.092(4)	0.611(3)	0.726(2)	370(9)
O2	0.1590(2)	0.80620(18)	0.90177(14)	153(3)
H21	0.076(4)	0.752(3)	0.935(2)	390(9)
H22	0.189(4)	0.859(3)	0.939(3)	410(9)
O3	0.4205(2)	0.69803(15)	0.75219(15)	143(3)
H31	0.506(3)	0.695(2)	0.701(2)	230(7)
H32	0.467(3)	0.684(3)	0.824(3)	380(8)
O4w	0.1727(3)	0.43274(18)	0.73808(16)	175(4)
H41w	0.118(3)	0.391(3)	0.717(2)	130(8)
H42w	0.264(4)	0.427(3)	0.720(3)	350(10)
O5w	0.5527(2)	0.6369(2)	0.96390(17)	210(4)
H51w	0.550(7)	0.578(4)	0.970(5)	130(2)
H52w	0.515(3)	0.683(3)	0.006(2)	140(7)
O6w	0.7400(2)	0.6737(2)	0.60933(16)	181(4)
H61w	0.745(4)	0.730(3)	0.547(3)	400(9)
H62w	0.737(4)	0.603(3)	0.599(3)	530(12)
O7w	0.9107(2)	0.62105(18)	0.01277(18)	197(4)
H71w	0.899(4)	0.614(3)	0.083(3)	350(9)
H72w	0.839(6)	0.634(5)	0.981(4)	110(2)
B1	0.7925(3)	0.0050(2)	0.7434(2)	114(5)
H1	0.854(3)	0.898(2)	0.7702(19)	200(6)
B2	0.5559(3)	0.0322(2)	0.7773(2)	112(5)
H2	0.465(3)	0.950(2)	0.8281(19)	160(6)
B3	0.6501(3)	0.0538(2)	0.6248(2)	120(5)
H3	0.618(3)	0.982(2)	0.5755(18)	140(5)
B4	0.8678(3)	0.1317(2)	0.6069(2)	117(5)
H4	0.981(3)	0.113(2)	0.5470(19)	190(6)
B5	0.9074(3)	0.1569(2)	0.7493(2)	120(5)
H5	0.044(3)	0.151(2)	0.7767(19)	190(6)
B6	0.7145(3)	0.0949(2)	0.8547(2)	126(5)
H6	0.725(3)	0.044(2)	0.954(2)	210(6)
B7	0.5220(3)	0.2002(2)	0.8043(2)	133(5)
H7	0.407(3)	0.220(2)	0.8694(19)	160(6)
B8	0.4836(3)	0.1753(2)	0.6620(2)	122(5)
H8	0.349(3)	0.182(2)	0.6352(19)	170(6)
B9	0.6762(3)	0.2364(2)	0.5578(2)	125(5)
H9	0.659(3)	0.286(2)	0.4628(19)	150(5)
B10	0.8344(3)	0.2998(2)	0.6340(2)	130(5)
H10	0.931(3)	0.388(2)	0.5864(18)	110(5)
B11	0.7400(3)	0.2783(2)	0.7874(2)	131(5)
H11	0.769(3)	0.350(2)	0.8377(19)	160(6)
B12	0.5984(3)	0.3265(2)	0.6677(2)	122(5)
H12	0.534(3)	0.431(2)	0.644(2)	230(6)

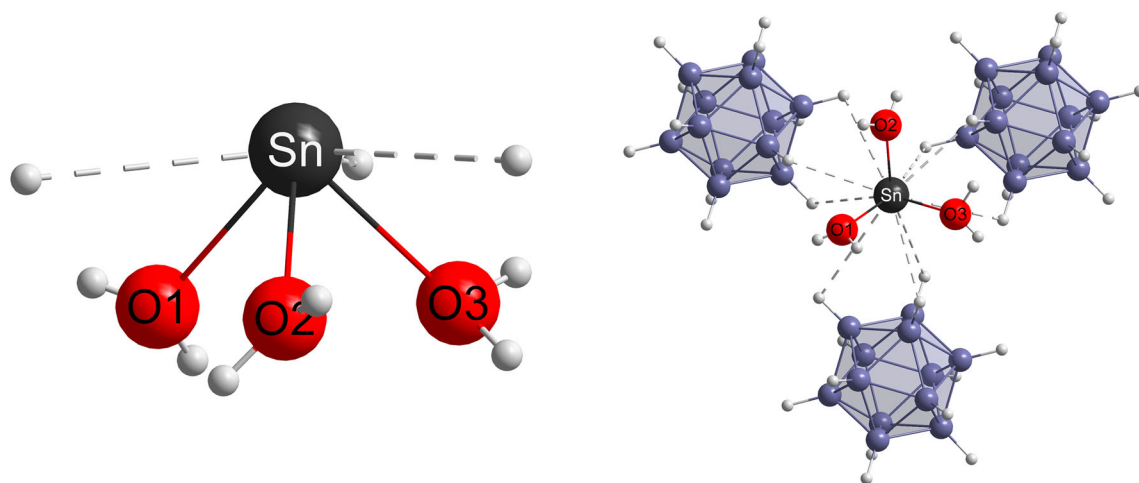


Fig. 5 First (left) and second coordination sphere (right) of the Sn^{2+} cations in $\text{Sn}(\text{H}_2\text{O})_3[\text{B}_{12}\text{H}_{12}] \cdot 4 \text{H}_2\text{O}$

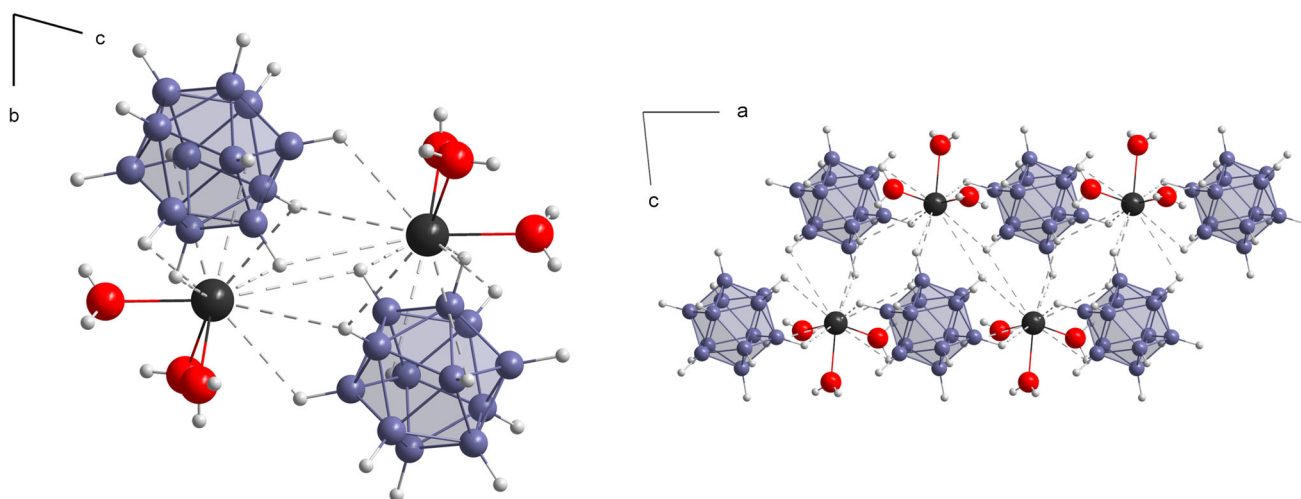


Fig. 6 View at the electroneutral double chains $\frac{1}{\infty} \{ \text{Sn}(\text{H}_2\text{O})_{3/1} [\text{B}_{12}\text{H}_{12}]_{3/3} \}$ as viewed along the propagating a -axis (left) and along $[010]$ (right) in $\text{Sn}(\text{H}_2\text{O})_3[\text{B}_{12}\text{H}_{12}] \cdot 4 \text{H}_2\text{O}$

longer than the Sn–H distance found in the metallacarborane [10-*endo*-(SnPh₃)-10- μ -*H*-7,8-*nido*-C₂B₉H₁₀][*trans*-Ir(CO)(PPh₃)₂(MeCN)], with $d(\text{Sn}-\text{H}) = 234 \text{ pm}$ [27], as well as the Sn–H contacts found in several dialkylstannylenes ($d(\text{Sn}-\text{H}) = 203\text{--}249 \text{ pm}$) [25, 26, 28, 29].

In the same way as the Pb^{2+} cations, Sn^{2+} cannot activate the B–H bonds, neither for the $[\text{B}_{12}\text{H}_{12}]^{2-}$ nor for the more reactive $[\text{B}_{10}\text{H}_{10}]^{2-}$ case. It seems that the desired B–H bond activation is only provided by Bi^{3+} cations and $[\text{B}_{10}\text{H}_{10}]^{2-}$ or $[\text{B}_{12}\text{H}_{12}]^{2-}$ anions [18, 19] under physiological conditions so far.

Experimental

$\text{Sn}(\text{H}_2\text{O})_3[\text{B}_{10}\text{H}_{10}] \cdot 3 \text{H}_2\text{O}$

The hydrated decahydro-*closo*-decaborate compound with divalent tin was yielded after the reaction of tin powder (99.9%, Fluka) with an excess of an aqueous solution of the free acid $(\text{H}_3\text{O})_2[\text{B}_{10}\text{H}_{10}]$, obtained by passing an aqueous solution of $\text{Cs}_2[\text{B}_{10}\text{H}_{10}]$ [30, 31] through a strong acidic ion-exchange column (Merck, Amberlite IR-120). After the hydrogen evolution has concluded, the resulting colorless solution was evaporated at 50 °C to dryness. The white precipitation was again dissolved in water, filtered to remove the remaining tin powder and evaporated

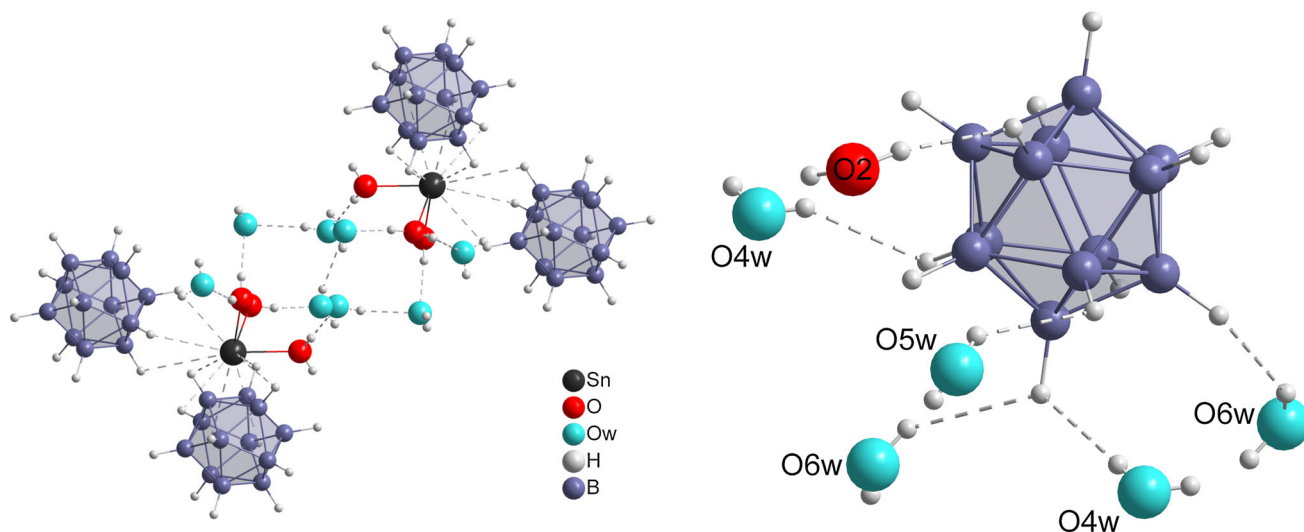


Fig. 7 Classical hydrogen bonds between two $\frac{1}{\infty} \{ \text{Sn}(\text{H}_2\text{O})_{3/1} [\text{B}_{12}\text{H}_{12}]_{3/3} \}$ chains (left) and the network of non-classical hydrogen bonds (right) in $\text{Sn}(\text{H}_2\text{O})_3[\text{B}_{12}\text{H}_{12}] \cdot 4 \text{H}_2\text{O}$

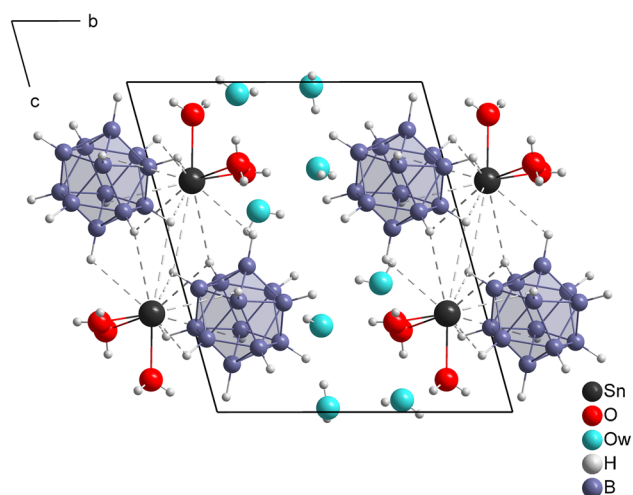


Fig. 8 View at the triclinic crystal structure of $\text{Sn}(\text{H}_2\text{O})_3[\text{B}_{12}\text{H}_{12}] \cdot 4 \text{H}_2\text{O}$ along [100]

isothermally at room temperature to obtain crystals within several days. The pristinely colorless and transparent tin(II) salt crystals with the $[\text{B}_{10}\text{H}_{10}]^{2-}$ anion, for being a much stronger reductant than $[\text{B}_{12}\text{H}_{12}]^{2-}$, becomes brown and opaque over time due to the continuous precipitation of colloidal tin.

$\text{Sn}(\text{H}_2\text{O})_3[\text{B}_{12}\text{H}_{12}] \cdot 4 \text{H}_2\text{O}$

The analogous $[\text{B}_{12}\text{H}_{12}]^{2-}$ salt was prepared by the reaction of tin powder (99.9%, Fluka) with an aqueous solution of the free acid $(\text{H}_3\text{O})_2[\text{B}_{12}\text{H}_{12}]$, obtained by passing an aqueous solution of $\text{Cs}_2[\text{B}_{12}\text{H}_{12}]$ [1, 32, 33] through a

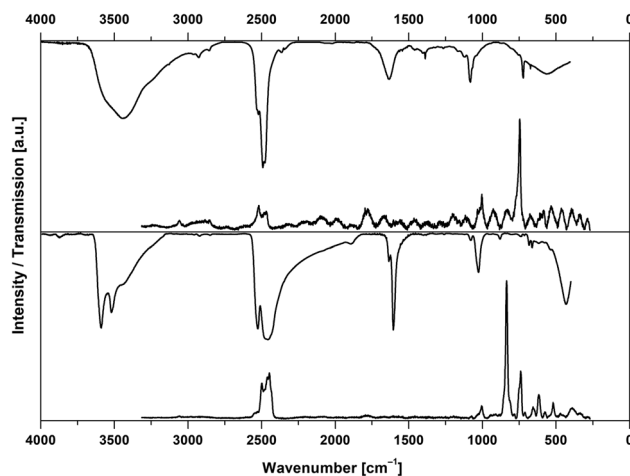


Fig. 9 Vibrational IR and Raman spectra of $\text{Sn}(\text{H}_2\text{O})_3[\text{B}_{10}\text{H}_{10}] \cdot 3 \text{H}_2\text{O}$ (bottom) and $\text{Sn}(\text{H}_2\text{O})_3[\text{B}_{12}\text{H}_{12}] \cdot 4 \text{H}_2\text{O}$ (top)

strong acidic ion-exchange column (Merck, Amberlite IR-120). The reaction solution was heated up to 50 °C for 2 days, filtered and then evaporated at room temperature to yield colorless single crystals within a few days.

An empirical absorption correction was performed by using the program *Scalepack* [34]. The crystal structure solutions and refinements were carried out with the program package *SHELX-97* [35]. Both structure refinements include the positions of all hydrogen atoms without any constraints. The coefficients of the equivalent isotropic displacement parameters are defined as $U_{\text{eq}} = \frac{1}{3} [U_{11}(aa^*)^2 + U_{22}(bb^*)^2 + U_{33}(cc^*)^2 + 2U_{12}aba^*b^*\cos\gamma + 2U_{13}aca^*c^*\cos\beta + 2U_{23}bcb^*c^*\cos\alpha]$ in pm^2 [36]. Further details of the crystal structure investigations may be

obtained from the CCDC (www.ccdc.cam.ac.uk) and FIZ Karlsruhe (www.fiz-karlsruhe.de) on quoting the depositary numbers 1872762 for $\text{Sn}(\text{H}_2\text{O})_3[\text{B}_{10}\text{H}_{10}] \cdot 3 \text{H}_2\text{O}$ and 1872763 for $\text{Sn}(\text{H}_2\text{O})_3[\text{B}_{12}\text{H}_{12}] \cdot 4 \text{H}_2\text{O}$.

The infrared spectroscopic data were measured as potassium-bromide powder pellets on a Bruker ALPHA FT/IR spectrometer (Bruker Optik GmbH, Ettlingen, Germany). Raman spectra of the single crystals were recorded by using a XploRA Raman microscope (HORIBA Jobin Yvon GmbH, Bensheim, Germany).

Acknowledgements We thank Dr. Falk Lissner and Dr. Sabine Strobel for the collection of the single-crystal X-ray diffractometer data. Furthermore, we like to thank Dr. Florian Ledderboge and Dipl.-Chem. Adrian H. Geyer for the single-crystal Raman measurements. We are also grateful to Dr. Katharina Bader from the group of Prof. Dr. Joris van Slageren (Institute for Physical Chemistry, University of Stuttgart) for the practical instruction to FT/IR measurements using potassium-bromide pellets.

Funding Open Access funding enabled and organized by Projekt DEAL.

Open Access This article is licensed under a Creative Commons Attribution 4.0 International License, which permits use, sharing, adaptation, distribution and reproduction in any medium or format, as long as you give appropriate credit to the original author(s) and the source, provide a link to the Creative Commons licence, and indicate if changes were made. The images or other third party material in this article are included in the article's Creative Commons licence, unless indicated otherwise in a credit line to the material. If material is not included in the article's Creative Commons licence and your intended use is not permitted by statutory regulation or exceeds the permitted use, you will need to obtain permission directly from the copyright holder. To view a copy of this licence, visit <http://creativecommons.org/licenses/by/4.0/>.

References

1. E. L. Muetterties, J. H. Balthis, Y. T. Chia, W. H. Knoth, and H. C. Miller (1964). *Inorg. Chem.* **3**, 444.
2. R. D. Dobrott and W. N. Lipscomb (1962). *J. Phys. Chem.* **37**, 1779.
3. T. E. Paxton, M. F. Hawthorne, L. D. Brown, and W. N. Lipscomb (1974). *Inorg. Chem.* **13**, 2772.
4. V. V. Avdeeva, A. E. Dziova, I. N. Polyakova, L. V. Goeva, E. A. Malinina, and N. T. Kuznetsov (2013). *Russ. J. Inorg. Chem.* **58**, 657.
5. E. A. Malinina, K. Y. Zhizhin, I. N. Polyakova, M. V. Lisovskii, and N. T. Kuznetsov (2002). *Russ. J. Inorg. Chem.* **47**, 1158.
6. V. V. Avdeeva, E. A. Malinina, I. B. Sivaev, V. I. Bregadze, and N. T. Kuznetsov (2016). *Crystals* **6**, 60.
7. I. Tiritiris, N.-D. Van, and Th. Schleid (2011). *Z. Anorg. Allg. Chem.* **637**, 682.
8. H. Kunkely and A. Vogler (2007). *Inorg. Chim. Acta* **360**, 679.
9. F. M. Kleeberg, L. W. Zimmermann, and Th. Schleid (2014). *Z. Anorg. Allg. Chem.* **640**, 2352.
10. E. A. Malinina, L. V. Goeva, and N. T. Kuznetsov (2009). *Russ. J. Inorg. Chem.* **54**, 417.
11. L. W. Zimmermann, F. M. Kleeberg, and Th. Schleid (2017). *Z. Anorg. Allg. Chem.* **643**, 365.
12. E. A. Malinina, K. A. Solntsev, L. A. Butman, and N. T. Kuznetsov (1989). *Koord. Khim.* **15**, 1039.
13. F. M. Kleeberg, *Doctoral Thesis* (University of Stuttgart; Dr. Hut, Munich, 2017).
14. K. Hofmann and B. Albert (2005). *Z. Kristallogr.* **220**, 142.
15. L.-L. Ng, B. K. Ng, K. Shelly, C. B. Knobler, and M. F. Hawthorne (1991). *Inorg. Chem.* **30**, 4278.
16. C. Nachtigal and W. Preetz (1996). *Z. Naturforsch. B* **51**, 1061.
17. C. Nachtigal and W. Preetz (1997). *Z. Naturforsch. B* **52**, 975.
18. L. W. Zimmermann, Ng. D. Van, D. Gudat, and Th. Schleid, (2016). *Angew. Chem. Int. Ed.* **55**, 1909.
19. L. W. Zimmermann, N.-D. Van, D. Gudat, and Th. Schleid (2016). *Angew. Chem.* **128**, 1942.
20. L. W. Zimmermann, *Doctoral Thesis* (University of Stuttgart; Dr. Hut, Munich, 2013).
21. G. R. Desiraju and T. Steiner, *The Weak Hydrogen Bond* (Oxford University Press, Oxford, 1999).
22. R. H. Crabtree, P. E. M. Siegbahn, O. Eisenstein, A. L. Rheingold, and T. F. Koetzle (1996). *Acc. Chem. Res.* **29**, 348.
23. J. A. Wunderlich and W. N. Lipscomb (1960). *J. Am. Chem. Soc.* **82**, 4427.
24. E. S. Shubina, E. V. Bakhmutova, A. M. Filin, I. B. Sivaev, L. N. Teplitskaya, A. L. Chistyakov, I. V. Stankevich, V. I. Bakhmutov, V. I. Bregadze, and L. M. Epstein (2002). *J. Organomet. Chem.* **657**, 155.
25. K. Izod, W. McFarlane, B. V. Tyson, I. Carr, W. Clegg, and W. R. Harrington (2006). *Organometallics* **25**, 1135.
26. K. Izod, C. Wills, W. Clegg, and R. W. Harrington (2009). *Organometallics* **28**, 2211.
27. J. Kim, S. Kim, and Y. Do (1992). *J. Chem. Soc. Chem. Commun.* **13**, 938.
28. K. Izod, C. Wills, M. R. Probert, and R. W. Harrington (2014). *Main Group Met. Chem.* **37**, 113.
29. K. Izod, C. M. Dixon, R. W. Harrington, and M. R. Probert (2015). *Chem. Commun.* **51**, 679.
30. D. A. Saulys, N. A. Kutz, and J. A. Morrison (1983). *Inorg. Chem.* **22**, 1821.
31. K. Vaas, *Doctoral Thesis* (University of Stuttgart, Stuttgart, 1999).
32. S. I. Uspenskaya, K. A. Solntsev, and N. T. Kuznetsov (1975). *Zh. Strukt. Khim.* **16**, 482.
33. I. Tiritiris, Th. Schleid, K. Müller, and W. Preetz (2000). *Z. Anorg. Allg. Chem.* **626**, 323.
34. Z. Otwinowski and W. Minor, *Scalepack: Program for Empirical Absorption Correction* (University of Texas at Dallas, Richardson, 1997).
35. G. M. Sheldrick, *SHELX: Program System for Crystal Structure Determination, Solution and Refinement from Diffractometer Data* (University of Göttingen, Göttingen, 1997).
36. R. X. Fischer and E. Tillmanns (1988). *Acta Crystallogr. C* **44**, 775.

Publisher's Note Springer Nature remains neutral with regard to jurisdictional claims in published maps and institutional affiliations.